Atom Indonesia

Journal homepage: http://atomindonesia.brin.go.id

Probabilistic Model of Liquefaction in Serpong and Its Impact on Nuclear Installation Safety

A. M. Haifani[1,2*], W. Prakoso[1], T. Setiadipura[2], H. Suntoko[2], A. G. Muhammad[3]

[1]*Department of Civil Engineering, Faculty of Engineering, University of Indonesia, Jl. Lingkar, Pondok Cina, Kecamatan Beji, Kota Depok, Jawa Barat 16424, Indonesia*
[2]*Research Centre for Nuclear Reactor Technology, Research Organization of Nuclear Energy, National Research and Innovation Agency, Serpong, South Tangerang, 40132, Indonesia*
[3]*Research Centre for Nuclear Material and Radioactive Waste Technology, Research Organization of Nuclear Energy, National Research and Innovation Agency, Serpong, South Tangerang, 40132, Indonesia*

ARTICLE INFO

Article history:
Received 30 April 2025
Received in revised form 9 August 2025
Accepted 20 August 2025

Keywords:

Nuclear Power Plant (NPP)
Liquefaction
Hazard analysis
Cyclic stress ratio
Probabilistic model

ABSTRACT

This study delivers the first full probabilistic liquefaction hazard assessment, filling a major gap in current geotechnical risk evaluation techniques for nuclear infrastructure. We want to assess liquefaction risk under seismic loading in the Serpong region, by integrating seismic hazard data and geotechnical site characteristics. The technique includes Probabilistic Seismic Hazard Analysis (PSHA), Ground Motion Prediction Equations (GMPEs), disaggregation curves, and soil characteristics extracted from 18 boreholes, such as SPT-N values, fines content, and groundwater level changes. Liquefaction triggering is assessed using Cyclic Stress Ratio (CSR), Cyclic Resistance Ratio (CRR), and associated factors (MSF, Rd), followed by probabilistic validation. Over a 50-year exposure period, the total liquefaction probability ranges from 0.5676 to 0.594, with the maximum vulnerability seen in water-saturated sandy layers at depths of 1-6 meters. These findings emphasize localized seismic susceptibility and have direct implications for risk-informed nuclear installation foundation design and regulatory safety evaluations. Furthermore, the findings can be integrated into Probabilistic Safety Assessment (PSA) frameworks to help with quantitative risk indicators like Core Damage Frequency (CDF) and Large Early Release Frequency (LERF). This study provides a reproducible methodology for assessing liquefaction at nuclear plants in other seismically active regions.

INTRODUCTION

The construction of Nuclear Power Plants (NPPs) in Indonesia, with the growing energy demand and pressure to mitigate the effects of climate change, has attracted great attention as a solution for energy diversification and carbon emission reduction [1]. However, the appropriate location of an NPP needs to be considered very carefully, especially in terms of safety. Liquefaction hazard analysis is an important part of site assessment as it can affect the stability and safety of infrastructure, including NPPs [2].

Liquefaction is a geotechnical phenomenon that occurs when earthquake vibrations weaken water-saturated soils and cause them to behave like a fluid [3]. Recent studies have shown that liquefaction is possible in the Tangerang region, especially in Serpong [4]. Serpong is at high risk due to its unique geology and requires a detailed liquefaction risk analysis. The region has thick and diverse sedimentary layers that may increase the risk of liquefaction [5]. A study by Hutabarat and Gahalaut confirmed the presence of water-saturated sand layers prone to liquefaction in some locations in Serpong [6]. To ensure the safety and sustainability of the operation of the planned nuclear power plant, the liquefaction potential needs to be carefully assessed. Well-known examples of the impacts of liquefaction include the large-scale damage in Niigata, Japan in 1964 and Christchurch, New Zealand in 2011 [7], Palu in 2016 [8].

*Corresponding author.
E-mail address: akhm020@brin.go.id
DOI: https://doi.org/10.55981/aij.2026.1676

Probabilistic liquefaction hazard analysis offers a more comprehensive method for risk assessment in such situations. To more accurately assess the probability of liquefaction, this probabilistic approach considers uncertainties associated with geotechnical and seismic ground loads [9-11]. This method also combines seismic and geotechnical data to develop models that can more effectively predict the possibility of liquefaction and its consequences. One of the main challenges in liquefaction hazard analysis is dealing with the large uncertainties and variability associated with soil properties and seismic parameters [12]. These variations include uncertainties in the magnitude, location, and depth of earthquakes, as well as differences in soil density, grain size distribution, and moisture content. These uncertainties make predicting earthquake stresses difficult. This can affect specific locations and impact the accuracy of the analysis. It is therefore important to develop techniques that can address these uncertainties.

The objective of this study is to address these uncertainties by constructing a probabilistic model to assess the liquefaction potential at Serpong and its impact on the safety of the nuclear installation. The model is expected to provide more accurate and reliable information for risk mitigation planning due to uncertain seismic parameters and ground properties. The results of this analysis will provide a better understanding of the liquefaction potential and effective mitigation strategies to minimize disaster risks, thereby supporting the development of a safe and sustainable nuclear power plant.

Novelty and contributions

This study makes a significant contribution to the advancement of liquefaction hazard analysis for Nuclear Power Plant (NPP) site safety in Indonesia. The key novelties are: Development and implementation of a comprehensive probabilistic liquefaction framework that systematically integrates seismic hazard parameters (PSHA, GMPEs, and hazard disaggregation) with geotechnical variability, accounting for both aleatory and epistemic uncertainties; First application of such a detailed model for the Serpong region, which is one of the designated candidate sites for future nuclear infrastructure. The resulting localized hazard profile provides critical input for site-specific planning, design, and regulatory compliance; Integration of liquefaction probability into the broader Probabilistic Safety Assessment (PSA) context, enabling quantitative risk estimation in terms of Core Damage Frequency (CDF) and Large Early Release Frequency (LERF) key metrics in nuclear safety evaluation.

Tectonic, geology, and geotechnics of Serpong

Serpong is located in a part of the very active seismic crust located in the subduction of South Java and active seismic crust units of mainland Java (West Java, West Java-Central Java-East Java). The active seismic fault traces in mainland Java are closely related to the presence of active fault structures, including the active seismic Banten fault trace, the active seismic Cimandiri fault trace, the active seismic Citarik fault trace, the active seismic Balibis fault trace, the active seismic tectonic Lembang fault trace, and the active seismic tectonic Citanduy fault trace [1] as shown in Fig. 1. As shown by continuous monitoring over 5 years (end of 2011 to July 2017), the seismic activity in Serpong does not indicate active tectonic setting [2].

Serpong's location is in an area close to active faults. There is a deep subduction zone in the north, the active Cimandiri fault at ±30 km away in the southeast, and the seismotectonic trace of the active Banten fault at ±40 km away in the west. Therefore, earthquakes caused by these faults are very likely to occur in this area. There have been several earthquakes in Serpong and its surrounding areas. On November 2, 1969, the epicenter distance was 52 km southeast of Serpong and was felt in the Kampaka Bogor V MMI area. On November 26, 1973, the epicenter distance was 63 km south of Serpong (scale V MMI), on 27 February 1903 with a hypocentral distance of 81 km northwest of Serpong (scale VI MMI), on 8 September 2012 with a hypocentral distance of 52 km south of Serpong (scale IV MMI), and on 8 August 2007 with a hypocentral distance of 108 km northeast of Serpong (scale V MMI).

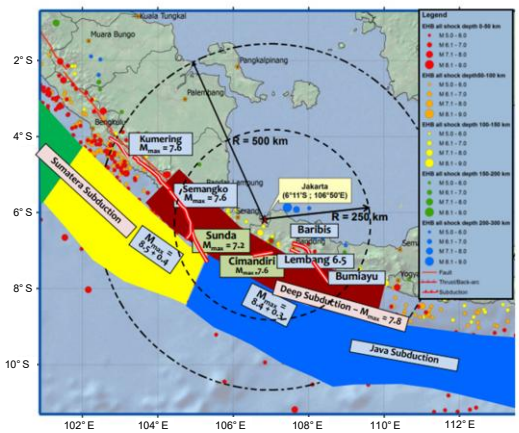

Fig. 1. Earthquake source zonation around the West Part of Java [13,14].

The Serpong area is located on a hilly plain at an altitude of 70-90 meters above sea level and has a variety of lithologies that may cause liquefaction phenomena. Based on the geological map [3], the area is composed of the Bojongmanik Formation, the Genteng Formation, the Serpong Formation, and alluvial deposits. The Bojongmanik Formation is composed of calcareous sandstone and mudstone with limestone intercalation, while the Genteng Formation is composed of pumiceous tuff, tuffaceous sandstone, and conglomerate with various lithological components. The younger Serpong Formation is composed of conglomerate with andesite and basalt components and unconformably overlies the Bojongmanik and Genteng Formations. The alluvial deposits covering the area are composed of clay, sand, and gravel. This lithology, especially alluvial deposits and calcareous sandstones with their granular nature, may increase the liquefaction potential when subjected to seismic loading and changing environmental conditions, as shown in Fig. 2.

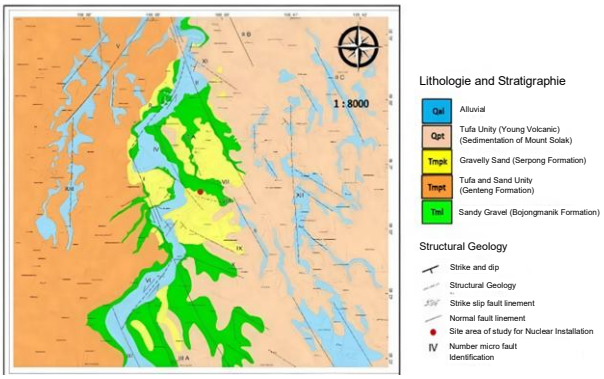

Fig. 2. Geological Area of 5 km from the centre of the study (modification [2]).

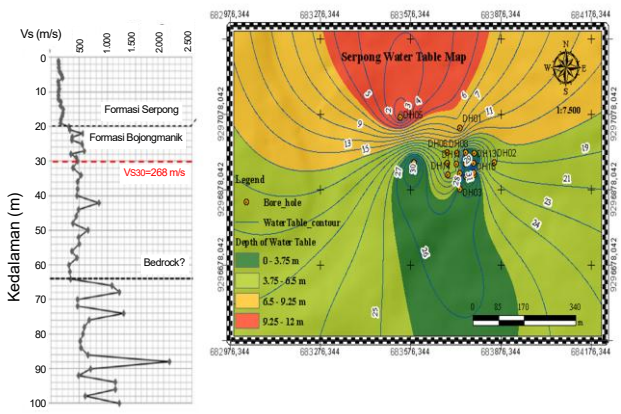

Fig. 3. a) VS Correlation with drilling data b) Groundwater depth distribution map dominated by depths between 3.76–6.5 m [15].

Geologically, the upper part of the Serpong area consists of layers of clay, clayey sand, sandy clay, loose to medium dense sand, dense sand, medium dense sand, and gravelly sand, which are part of the serpong formation. The lower part is part of the bojongmanik formation, consisting of thin layers of mudstone, clayey sandstone, sandy mudstone, and clastic limestone. Based on the results of cross-hole (inter-hole) seismic measurements, the average vs value at a depth of 30 meters is 268 m/s, and the average spt is 40.6.

The spt test is performed by dropping a hammer from a height of 76 cm. The test results show that the spt values are low or included in the sandy soils at a depth of ± 3 to 18 m, including soft to medium soils on the residual soil, and loose-dense soils at a depth of 18 m or more according to available data, approaching the layer boundary of mudstone, which is part of the bojongmanik formation [15]. The shallow groundwater table in the serpong area has a high potential for liquefaction as shown in Fig. 3.

METHODOLOGY

Probabilistic seismic hazard analysis

PGA values for six return periods (100, 250, 500, 1000, 2500, and 5000 years) were obtained from a site-specific probabilistic seismic hazard analysis (PSHA) of the Serpong region, which used standard GMPEs [4] and regional seismic sources around 500 km from the site area (Fig. 1). These numbers were used to calculate the cyclic stress ratio (CSR) in liquefaction study. Table 1 outlines the adopted PGA values.

Table 2 summarizes the key geotechnical and seismic parameters adopted for the liquefaction assessment in the Serpong area. The data were compiled from 18 borehole log points [15] and estimated through seismic wave propagation modelling using 175 global earthquake records. The estimation considers the disaggregation curves to define representative distance and moment magnitude (Mw) as proxies for the most critical seismic sources likely to cause damage in the study area. The range of parameters, including peak ground acceleration, fines content, corrected SPT values, and factor of safety, integrates field investigation results, classic empirical correlations [5-7], and probabilistic seismic hazard analyses (PSHA), ensuring the reliability and comprehensiveness of the liquefaction hazard evaluation.

Table 1. Seismic hazard levels (PGA) adopted for liquefaction analysis.

Return Period(Years)	Peak Ground Acceleration (PGA – g)
250	0.072
500	0.152
1000	0.236
2500	0.351
5000	0.456

Table 2. Geotechnical parameterisation for assessing liquefaction hazard from 18 boreholes at Serpong site.

Parameter	Symbol/ Unit	Value	Source / Referrence
Depth	(m)	0 - 30	Borehole log [2]
Peak Ground Acceleration	amax (g)	0.158 - 0.7	PSHA results, Stewart et al. (2003) [22]
Moment Magnitude	Mw	5.25 - 9	Disaggregation curve [35]
Distance	(km)	15 - 285	Disaggregation curve [35]
Fines Content	FC (%)	17.64 - 37.3	Borehole log [2]
N-SPT Correction	N_{1_60}	8.6625 - 25.8364	Borehole log [2]
Initial Eff	kPa	54 - 377	Borehole log [2]
Cyclic Stress Ratio	CRR	0.04 - 0.966	Youd, T. L., & Idriss, 2001 [5]
Cyclic Resistance Ratio	CSR	0.135 - 0.306	Andrus & Stokoe (2001) [13]
Factor of Safety	FS	0.19 - 4.78	Youd, T. L., & Idriss, 2001 [5]
Liquefaction Potential Index	LPI	0 - 7.44	Iwasaki (1982) [36]
Magnitude Scalling Factor	MSF	0.78 - 2.49	Seed et al., 1987 [14]
Stress Reduction Coefficient	Rd	0.264 - 1	Cetin & Seed (2004) [20]

In the absence of site-specific proprietary nuclear design data, this study uses a generic nuclear power plant foundation configuration based on international safety standards and engineering best practices. The assumed design includes a mat or piled raft foundation system with end-bearing piles extending to non-liquefiable strata, which is typical of standard NPP configurations in high seismic zones [8,9]. These assumptions enable a conservative yet realistic assessment of the soil-structure interaction and liquefaction-induced deformation impacts during extreme seismic loading.

Calculation of cyclic stress ratio

Cyclic stress ratio is the magnitude of earthquake stress and is expressed as the ratio of saturated soil shear stress to effective soil stress. The main component of CSR is to determine the maximum ground acceleration at the surface. Cyclic Stress Ratio (CSR) is a parameter that describes the stress distribution that controls the soil layer. CSR is a function of the maximum ground acceleration at the surface, the nonlinear soil mass participation factor, and the ratio of effective normal stress to total soil stress at the desired depth [16].

CSR is the ratio of cyclic voltage to total voltage. The lower the total overlay voltage, the smaller the CSR value. The total stress is a function of depth. A simplified procedure was first introduced by Seed and Idriss in 1971 using the Standard Penetration Test (SPT) strike number. It is related to cyclic loading of soils and is called the cyclic stress ratio [17,18]. The deeper the soil layer under consideration, the higher the total stress value. The analysis was carried out using the CSR evaluation formula proposed by Seed and Idriss [10] and S. L. Kramer and R. T. Mayfield [19] as follow Eq. (1):

$$CSR_{M=7.5,\sigma'_v=1\ atm} = 0.65\ \frac{a_{max}}{g}\frac{\sigma_v}{\sigma'_v}\frac{1}{Rd.MSF} \qquad (1)$$

Where csr is the cyclic stress ratio, a_(max) is the maximum ground acceleration at the ground surface, g is the gravitational acceleration, rd is the stress reduction factor, msf is a scaling factor considering the duration of the shaking effect, σ_v is the total stress, and σ'_v is the effective stress.

The magnitude scaling factor (MSF) is 1 for an earthquake with a magnitude of 7.5. For magnitudes other than 7.5, the MSF can be defined as a multiplier for the earthquake magnitude on a moment scale equal to CRR 7.5. The magnitudes of an earthquake play a role in analyzing liquefaction. The greater the magnitude of the earthquake, the greater the potential for soil liquefaction. Several researchers have proposed correction values for the MSF [10-14]. One of the equations used in MSF calculations in Eq. (2) [15]:

$$MSF = 1 + (MSF_{maks} - 1)\left(8.64\exp\left(\frac{-M}{4}\right) - 1.325\right) \qquad (2)$$

Magnitude Scaling Factor (MSF) is calculated using an equation as Eq. (3):

$$MSF_{maks} = 1.09 + \left(\frac{q_{c1Ncs}}{180}\right)^3 \leq 2.2 \qquad (3)$$

The equation used to calculate the stress reduction coefficient (rd) is based on the formulation proposed by Cetin, incorporating several predictive variables that influence the rd value, such as depth (m), moment magnitude (Mw), peak ground acceleration at the surface (amax), and average shear-wave velocity in the upper 12 meters (Vs12) Eq. (4).

In the formula, d represents depth in meters (m), amax denotes the peak ground acceleration, Vs12 is the average shear-wave velocity in the upper 12 meters expressed in meters per second (m/s), and e denotes the base of the natural logarithm (Euler's number).

$d \geq 20m\ (\sim 65\ ft)$

$$r_d(d, M_w, a_{max}, V*_{12m}) = \frac{\left[1 + \frac{-23.013 - 2.949a_{max} + 0.999M_w + 0.0525V*_{s,12m}}{16.258 + 0.201e^{0.341(-20+0.0765V*_{s,12m}+7.586)}}\right]}{\left[1 + \frac{-23.013 - 2.949a_{max} + 0.999M_w + 0.0525V*_{s,12m}}{16.258e^{0.341(0.0765V*_{s,12m}+7.586)}}\right]} - 0.0046(d-20) \pm \sigma_{\varepsilon r_d}$$

$d < 12\ m(\sim 40\ ft)\quad d \geq 12m(\sim 40\ ft)$

$$\sigma\ (d) = d^{0.850}0.0198\quad \sigma_{\varepsilon r_d}(d) = 12^{0.850}0.0198 \tag{4}$$

$d < 20\ m\ (\sim 65\ ft)$

$$r_d(d, M_w, a_{max}, V*_{12m}) = \frac{\left[1 + \frac{-23.013 - 2.949a_{max} + 0.999M_w + 0.0525V*_{s,12m}}{16.258 + 0.201e^{0.341(-d+0.0765V*_{s,12m}+7.586)}}\right]}{\left[1 + \frac{-23.013 - 2.949a_{max} + 0.999M_w + 0.0525V*_{s,12m}}{16.258e^{0.341(0.0765V*_{s,12m}+7.586)}}\right]} \pm \sigma_{\varepsilon r_d}$$

Calculation Cyclic Resistance Ratio (CRR) evaluation

The Cyclic Resistance Ratio (CRR) represents the soil's capacity to resist shear stress during an earthquake. When the induced shear stress exceeds the CRR, soil liquefaction may occur. CRR can be evaluated through either laboratory or field testing (Robertson and Wride, 1998). Common field tests used to assess CRR include the Standard Penetration Test (SPT), Cone Penetration Test (CPT), shear wave velocity (Vs) measurements, and the Becker Penetration Test (BPT). Laboratory assessments typically involve cyclic triaxial and direct shear tests.

In this study, CRR was evaluated based on shear wave velocity (Vs) measurements. The use of Vs as an index of liquefaction resistance is well justified, as both Vs and liquefaction resistance are influenced by similar factors, such as void ratio, stress state, stress history, and geologic age.

The correlation for CRR is developed by adjusting the Cyclic Stress Ratio (CSR) values from historical earthquake case studies to a reference magnitude of Mw = 7.5, equivalent to a cyclic stress ratio with a normalized clean sand value of Nc = 15 and an effective overburden stress σ′vo = 100 kPa, using CPT and SPT-based data ($CSR_{M=15,\sigma'_v=1=100} = CRR_{M=7.5,\sigma'_v=1}$). The CRR value is determined using the following Eq. (5):

$$CRR_{M=7.5,\sigma'_v=1\ atm} = exp\left(\frac{q_{c1Ncs}}{113} + \left(\frac{q_{c1Ncs}}{1000}\right)^2 - \left(\frac{q_{c1Ncs}}{140}\right)^3 + \left(\frac{q_{c1Ncs}}{137}\right)^4 - 2.8\right)$$

$$CRR_{M=7.5,\sigma'_v=1\ atm} = exp\left(\frac{N_{1\_60cs}}{14.1} + \left(\frac{N_{1\_60cs}}{126}\right)^2 - \left(\frac{N_{1\_60cs}}{23.6}\right)^3 + \left(\frac{N_{1\_60cs}}{25.4}\right)^4 - 2.8\right) \tag{5}$$

The detailed procedure for CRR calculation follows the methodology proposed by Robertson [16].

Calculation Factor of Safety (FS)

The Factor of Safety (FS) is a key parameter used to evaluate whether a site is susceptible to liquefaction [17,18]. FS is defined as the ratio between Cyclic Resistance Ratio (CRR) and Cyclic Stress Ratio (CSR), and serves as an indicator of liquefaction potential. When FS < 1, the soil is considered potentially susceptible to liquefaction; conversely, FS>1 indicates that liquefaction is unlikely to occur.

In this study, the factor of safety was calculated using the CPT-based liquefaction triggering procedure proposed by Boulanger and Idriss [15], as follows Eq. (6):

$$FS = \frac{CRR_{M=7.5,\sigma'_v=1\ atm}}{CSR_{M=7.5,\sigma'_v=1\ atm}} \tag{6}$$

Total probability analysis of liquefaction

Generally, there are two scenarios for probability calculations. The first scenario is a reanalysis of the post-earthquake events using a pair of seismic parameters (a_{max}, Mw). Data are obtained from earthquake records in a specific area and are used to evaluate soil liquefaction in the study area. The second scenario is a prospective analysis, i.e. design scenarios or seismic parameters related to a specific seismic hazard level (475). The probabilistic analysis of liquefaction uses a total probability approach [10] by comparing the results with the probability theory approach [21].

The total liquefaction probability theory explains the distribution of earthquake parameters in the form of amax and Mw, which contribute to

determining the magnitude of liquefaction probability. This theory states as a product of conditional probability, the probability of liquefaction occurring when the event estimates the combination of amax and Mw [10,11]. This approach describes the sum of the probability weights of each earthquake parameter described in the following formula Eq. (7):

$$P_{LT} = \sum_{Allpairsof\,(a_{\max},M_w)} \{p[L\,|\,(a_{\max},M_w)].p(a_{\max},M_w)\} \quad (7)$$

where the term p[a_max | PGA>h] is the conditional liquefaction probability explaining the probability of a_{max} occurring when the likelihood of a PGA > H occurs due to an accident, p(a_{max},M_w) is a joint probability between a_{max} and Mw, or the possibility of an $a_{max}$and Mw parameter, which can occur coincidently. Meanwhile, a product of p[a_{max} | PGA>h] dan p(a_max,M_w) is expressed as a weighted probability or also known as the weighted consequences of a single occurrence. The summation of the probability weighting produces a total probability of liquefaction, which can be regarded as expected in the designated area. Equation (7) implied that the possibility of liquefaction depends only on a_{max} and Mw. This assumption is fundamental to all cyclic stress-based method that follow the simplified procedure developed by Seed [10]. This assumption is also considered acceptable since the simplified approach has been calibrated with case histories where the liquefaction potential is conditioned only on a_{max} and Mw. The value of earthquake acceleration (a_{max}) is obtained by using a calculation approach of the site [22] with the scheme as follows Eqs. (8,9):

Define amplification factor (F):

$$\ln(F) = a + b\,(PGA) + \boldsymbol{\varepsilon} \quad (8)$$

Define a_{max} based on amplification factor (a_{max}):

$$\begin{aligned} \ln(amax) &= \ln(F) + \ln(PGA) \\ &= [a + bln(PGA) + \varepsilon] \\ &+ ln(PGA) \end{aligned} \quad (9)$$

where parameters a and b are regression coefficients. For example, for alluvial deposits (Qa) in the secondary deposition category, a = -0.15 and b = -0.13. The error term ε is calculated as a normally distributed random variable with mean zero ($\tilde{\varepsilon}$=0) and standard deviation $\sigma\boldsymbol{\varepsilon}$ =0,52 (for Qa storage). The value of ln(a_{max}) obtained from Eq. (9) is considered as a normally distributed random variable when the error term ε = standard random variable. The mean of ln(a_{max}) depends on the PGA value when the standard deviation of ln(a_{max}) for alluvial deposits Qa is equivalent to 0,52 [22].

Conditional probability of liquefaction $p[a_{max}|PGA > h]$

Several probability function formulas based on regression-based methods [23,24] can be used as a reference, including reliability analysis and Monte Carlo simulation [11,24]. The Use of the logistic regression method to obtain the probabilistic field boundary curve proves the initiation of liquefaction, which includes effective overburden pressure, a fixed number of SPT blows, and FC [25]. As a result of a fully probabilistic verification of the liquefaction hazard [10], this study uses two approaches that have been previously proposed by several researchers. The first validation is a calculation carried out using the Poisson distribution approach. A study using a probabilistic method in calculating conditional probability [23] as the Possibility of Liquefaction (PL), which can be expressed as Eq. (10):

$$P_L = \Phi\left[-\frac{(N1)_{60}(1+\theta_1 FC) - \theta_2 lnCSR - \theta_3\, lnMw - \theta_4 \ln\left(\frac{\sigma'_v}{Pa}\right) + \theta_5 FC + \theta_6}{\sigma_\epsilon}\right] \quad (10)$$

where Φ is the standard normal cumulative distribution function, $(N1)_{60}$ is the 60% corrected SPT resistance, FC is the fines content (in percent), CSR_{eq} is the cyclic stress ratio, Mw is the moment magnitude, σ'_v is the initial effective overburden pressure, σ_ϵ is the size of the model estimate and parameter uncertainty, dan θ_1– θ_6 are the model coefficients obtained through regression. The second validation adopts an equation based on the nonlinear regression approach [24,25].

a. Jafarian 2011: $P_L = \frac{1}{1+3.13F_S{}^{2.735}}$ (11)

b. Juang 2002: $PL = \frac{1}{1+\left(\frac{FS}{0.36}\right)^{4.8}}$ (12)

Liquefaction hazard is estimated to occur when FS values < 1. Probabilistic analysis uses earthquake recurrence periods and annual incidence rates of liquefaction to estimate liquefaction [19]. A Poisson process is assumed to be the probability of multiple earthquake events that can cause liquefaction at a particular level and occur at a certain time or spatial interval. The earthquake events have known independent time-averaged

rates that are constant since the last earthquake. The probability of liquefaction for an exposure time of T = 50 can be converted from annual liquefaction rates to probabilistic liquefaction using the following Eqs. (13-16):

$$P_{LTP} = 1 - e^{\lambda_{P_{LT}} T_{amax,Mw}} \quad (13)$$

$$\lambda_{P_{LTP}} = \sum_{i=1}^{amax} \sum_{j=1}^{Mw} P_{LT} \triangle \lambda_{amax_i, Mw_j} \quad (14)$$

$$\triangle \lambda_{amax_i, Mw_j} = \frac{-ln(1 - p(a_{max} Mw, 1))}{T(1)} - \frac{-ln(1 - p(a_{max} Mw, 7))}{T(7)} \quad (15)$$

Where P_{LTP} is the sum of probabilistic liquefaction volumes based on a poisson distribution, s the annual mean liquefaction volume, is the additional annual mean exceedance rate of strength measurements, and magnitudo, is the predicted recurrence value of liquefaction assuming 10% occurrence within a 50-year exposure period, t(1) and t(7) are the shortest and longest recurrence periods of liquefaction for earthquakes with values of 224 and 975 years.

The joint distribution between a_{max} and Mw

The procedure for performing a joint distribution between a_{max} and Mw is as follows:
Determine the joint probability between amax, mw, and pga>h (h hazard level), which is expressed as; Determine the joint probability between amax, mw, and h for each hazard level, which is expressed as; Determine the probability mass function between amax and Mw and express as:

Joint probability amax, Mw, PGA>h as:

$$p(a_{max}, Mw, PGA > h) = p(a_{max} | (Mw, PGA > h). p(Mw | PGA > h). p(PGA > h) \quad (16)$$

where $p(a_{max}, Mw, PGA > h)$= joint probability of three events, a_{max}, *Mw* dan *PGA>h*. $p[a_{max}|Mw, PGA > h]$ = conditional probability a_{max} given Mw dan PGA>h, *p*(Mw|PGA>h) = conditional probability Mw is given PGA>h (Mw distribution is extracted from disaggregation curve), and *p*(PGA>h) = probability of PGA exceeding with certain hazard level as shown in Fig 4.

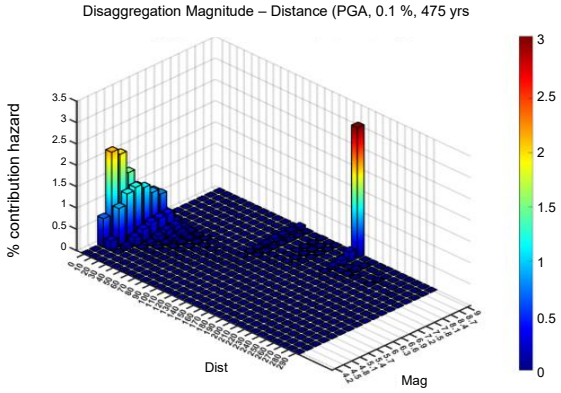

Fig. 4. Dissagregation curve for the Serpong area with the highest hazard contribution to the earthquake source at 210 km and 9 magnitude.

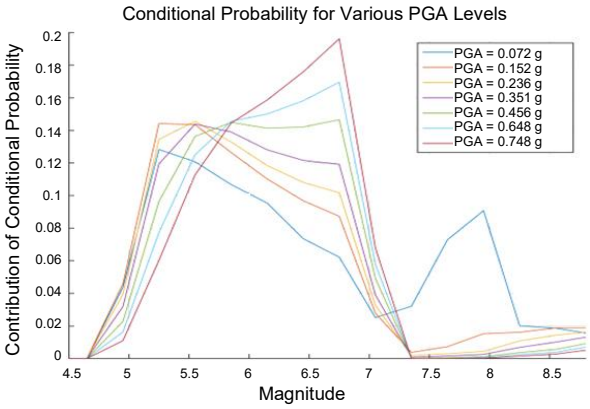

(a)

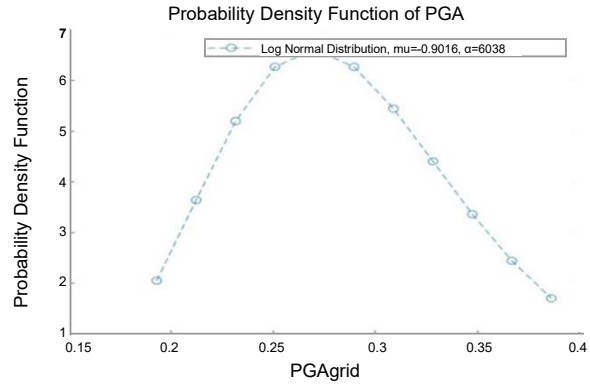

(b)

Fig. 5. (a) Conditional probability for 6-level hazard, (b) Probability density function for various hazard levels at Serpong.

The P (PGA > h) value is derived from describing in Fig. 5(a) the distribution of PGA values at the base rocks based on the six hazard levels used in the PSHA analysis in the research area. The probability value is calculated based on the area covered in Fig. 5(b), assuming a continuous distribution. The value of p (Mw | PGA > h) is the probability of Mw given of PGA > h.

Conditional probability values that are mentioned with $p[amax|Mw, PGA > h]$ are a conditional probability of a_{max} given Mw and PGA > h. These values can be replaced with $p[amax|PGA > h]$ because the value of a_{max} depends on PGA > h, and it does not use Mw. To obtain the value of a_{max} refers to the concept of amplification factor, stated in Eqs. (17) [22]

Conditional probability a_{max} has given Mw and PGA>h, $(p(a_{max}|Mw, PGA > h))$

$$p(a_{max}|Mw, PGA > h) = p(a_{max}|PGA > h) \quad (17)$$

by using conditional probability definitions, then the value of p[a_{max} |PGA>h] can be determined by the as follow Eq. (18):

Conditional probability a_{max} has given PGA>h, ($p[a_{max}|PGA > h]$)

$$p[a_{\max} \mid PGA > h] = \frac{p(a_{\max,} PGA > h)}{p(PGA > h)} \quad (18)$$

where p(a_{max}, PGA>h) is a joint probability between a_{max} dan PGA>h, which is defined by the as follows Eq. (19):

Sum Joint Probability between a_{max} and PGA

$$p(a_{\max}, PGA > h) = \sum_{PGA=h+\Delta PGA}^{u} p(a_{\max}, PGA) \quad (19)$$

where p(a_{max}, PGA) is the joint probability of a_{max} dan PGA, which is estimated by the equation $p(a_{max}, PGA) = p(a_{max}|PGA).p(PGA)$. The p(a_{max}|PGA) is available from Eq. (20). Then, the joint probability of a_{max} dan PGA can be calculated by using the as follow Eq. (20):

Joint probability between a_{max} and PGA, $(p(a_{max}, PGA))$

$$p(a_{max}.PGA) = \left\{ \frac{1}{a_{max}\sigma_{ln(a_{max})}\sqrt{2\pi}} exp\left[\frac{-\{ln(a_{max}) - \mu_{ln(a_{max})}\}^2}{2\sigma^2_{ln(a_{max})}} \right] \right\}_{\Delta a_{max}} . p(PGA) \quad (20)$$

where $\mu_{\ln(amax)}$ =a+(b+1) * ln (PGA) dan a=-0.15, b=-0.13 and $\sigma_{\ln(amax)}$= σ_ϵ for Qa deposits refer to Stewart et al. [22]. The values $\mu_{\ln(amax)}$ dan $\sigma_{lan(amax)}$ are two distribution parameters of the log normal distribution of a_{max} and PGA.

Joint probability a_{max}, Mw, and h for any hazard level.

At stage one, set the joint probability *p(a_{max}, Mw, PGA>h)* by implementing Eq. (21). The second stage is to set the joint probability of a_{max}, Mw, and h (for any level of PGA) notified as *p(a_{max}, Mw,h)* with the equation such as:

$$p(a_{max}, M_w, h) = p(a_{max}, M_w, PGA > h) - p(a_{max}, M_w, PGA > h + \Delta PGA) \quad (21)$$

The joint probabilities are defined for all possible combinations of hazard levels.

Define probability mass function $a_{max}$and Mw, $(p(a_{max}, Mw))$

The joint probability mass function is assumed to be the probability of a random occurrence of a_{max} and Mw, which is calculated with P (a_{max}, Mw) by summing up the joint probability $p(a_{max}, M_w, PGA > h)$. Eq. (22) expresses this probability.

$$p(a_{\max}, M_w) = \sum_{h}^{p} (a_{\max}, M, h) \quad (22)$$

RESULTS AND DISCUSSION

Serpong area, Tangerang Province, Indonesia is a location that has the potential for liquefaction hazards. The soil parameters used at a depth of 9 m in the Qa area are N_{1_60} = 3.47, FC = 93.58, = 201 = 176.4. The joint probability curve (Fig. 6a) based on the a_{max} and Mw pairs shows that a_{max} the range between 0.09 and 0.5 g and Mw with a range of 6.5 - 7.9 dominates the joint probability distribution between a_{max} and Mw, with peaks at 0.23 g and 7.8. The total liquefaction probability uses the conditional liquefaction approach from the Cetin model. [20]. Fig. 6b shows the conditional liquefaction probability distribution. The weighted liquefaction probability for each a_{max} and Mw pair is proportional to the joint liquefaction probability (Fig. 6(d)) and the conditional liquefaction probability. Conditional probability is calculated using the equation [20]. Fig. 6d shows the weighted liquefaction probability distribution. The entire volume of weighted liquefaction distribution produces a total probability of liquefaction occurring within a 50-year exposure time with a PLT value of 0.5676.

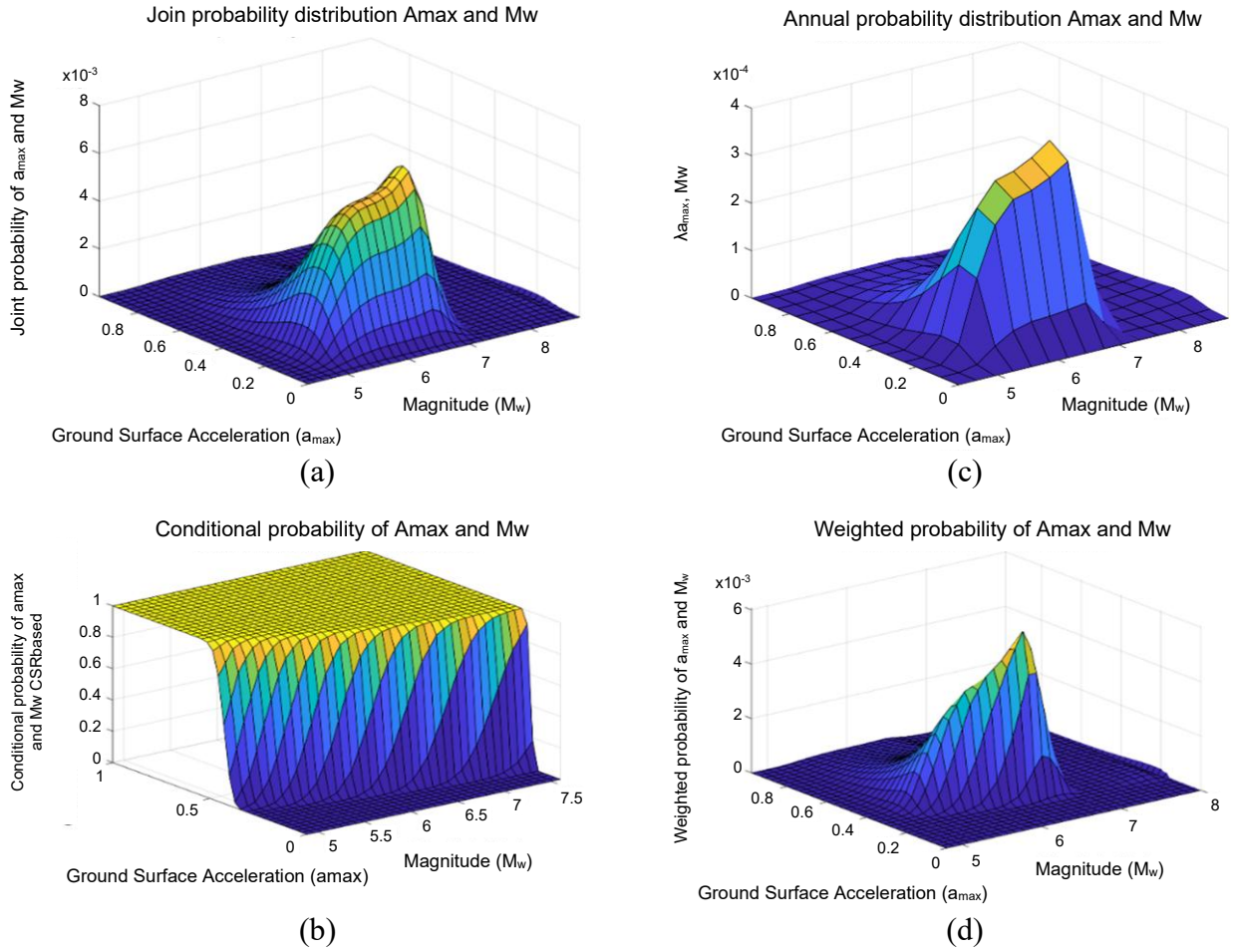

Fig. 6. a) Joint probability distribution, b) Conditional probability distribution, c) Annual probability rate distribution between a_{max}dan Mw for Serpong, Tangerang, Indonesia, and d). weighted probability distribution.

Table 3. Comparison of probabilistic liquefaction hazard calculations.

Probability Method	Total Probability Combination Cetin 2004, Juan 2006	Annual Probability Rate Krammer 2006	Liquefaction Probability Jafarian 2010	Liquefaction Probability Juang 2002
Liquefaction Probability (P_{LT})	0.5676	0.5940	0.5748	0.5839

Based on the poison distribution approach, the annual liquefaction rate of the study area λ = 0.007 is generated from the Kramer equation [19]. The liquefaction probability with a 50-year exposure time is converted from the annual liquefaction rate to produce PLT = 0.594. This value is compared with the calculation using the equation from Juan [10]. The Juang 2002 equation has a probability value that is close to the total probability estimate, which is explicitly 0.5839. The analysis also uses the probability approach proposed by Jafarian 2010, Equation [18] for PLT exposure time of 50 years = 0.5748. The results of this calculation are quite comparable to the Kramer 2006 equation estimate and the analytical work of Equation [16] proposed by Juang 2006 by elaborating the Cetin model equation as the evaluation stage of the calculation [20]. The comparison can be seen in Table 3.

The liquefaction hazard in the Serpong area is illustrated in the liquefaction distribution map. This map shows that the probability values are relatively uniform across the area. This uniformity arises from the limited spatial coverage of borehole data, leading to the assumption that the soil lithology is consistent throughout the region. The probability values are calculated based on an assumed 500-year earthquake recurrence period, which serves as the standard for civil engineering and architectural design.

Figure 6 (a, b, c, and d) illustrates the liquefaction probability for depths ranging from 1 to 6 meters, with earthquake magnitudes of 4.5, 5.0, and 6.5 Mw. The results indicate that the overall probability remains relatively low, with a maximum value of 24%. However, the data show that both the likelihood of liquefaction and the affected area increase as the earthquake magnitude rises. For an

earthquake magnitude of 4.5 Mw, the liquefaction probability ranges from 0.729 to 0.966, affecting approximately 0.8 square meters. As the magnitude increases to 5.0 Mw, the maximum probability rises to 0.809–0.979, with the affected area expanding to 15 square meters. At a magnitude of 6.5 Mw, the maximum probability reaches 0.874–0.995, with the affected area increasing to 17 square meters. These results highlight that the susceptibility of the soil to liquefaction significantly increases with higher earthquake magnitudes.

In addition, liquefaction consistently occurs at depths of 1 and 6 meters, indicating that the soil at these depths is particularly vulnerable to liquefaction. The nuclear installation site in Serpong is susceptible to liquefaction at these same depths. In the central area of the Serpong site, the liquefaction probability reaches as high as 98% at a magnitude of 8 Mw, highlighting the critical need for mitigation measures. The probability values demonstrate a linear relationship with earthquake magnitude, where higher magnitudes result in higher liquefaction probabilities.

At a depth of 6 meters, the spatial distribution of liquefaction susceptibility aligns with the river flow, suggesting that soils along the riverbanks composed of uniform sand grain sizes and unconsolidated deposits are more prone to liquefaction. The elevated probability in the central part of the study area is further supported by the shallow groundwater levels, as shown in Fig. 3(b). The figure indicates that groundwater depths in the study area range between 0 to 6.5 meters, with the most common depth at 3.75 meters or lower. According to Budhu (2010), groundwater in this range is classified as very shallow to shallow, increasing the soil's vulnerability to liquefaction [37]. As Kramer (1996) suggests, the susceptibility to liquefaction decreases with deeper groundwater levels, but locations with groundwater close to the surface remain highly susceptible. Fluctuations in surface elevation can also lead to variations in liquefaction hazards [18].

The results of the liquefaction probability analysis are illustrated in Fig. 7, which shows the distribution of liquefaction probability across Serpong for a 500-year return period. The scenarios include earthquakes with magnitudes of 4.5, 5.0, and 6.5 Mw at a depth of 6 meters. The green symbols on the map represent borehole locations (e.g., DH01 to DH20), which provide the soil data used in the liquefaction susceptibility analysis. The color gradient on the map reflects the probability levels, with light green representing low probability and pink to purple indicating high probability.

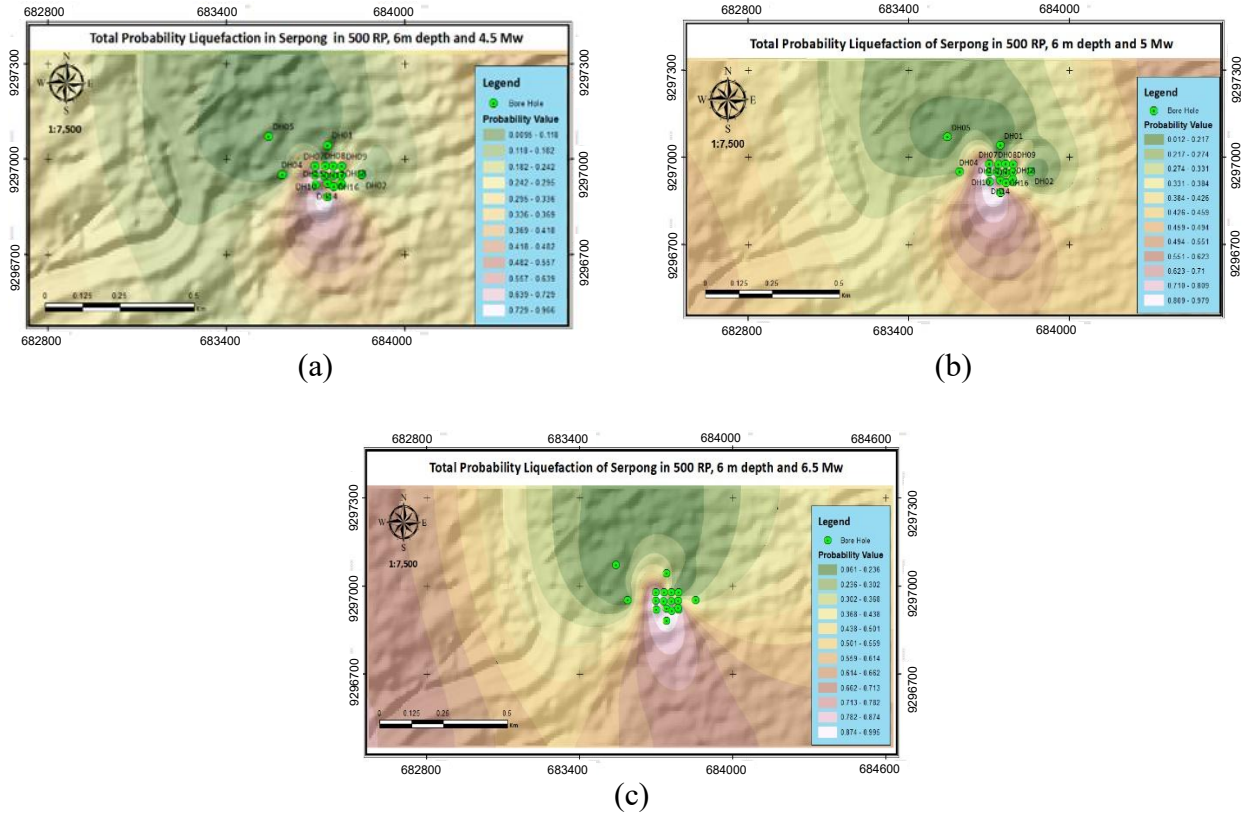

Fig. 7. Liquefaction Probability in Serpong in 500 RP for a) 6m, 4.5 Mw b) 6m, 5 Mw and c) 6m, 6.5 Mw.

Based on the probability calculations, the liquefaction probability at the Serpong site ranges between 0.5676 and 0.594 over a 50-year period. This level of risk requires serious consideration in the planning and mitigation efforts for the site. Such probabilities indicate a significant likelihood of foundation settlement or structural deformation, particularly during a major earthquake [9]. In the operation of a nuclear power plant, these disruptions could lead to malfunctions in cooling and control systems, posing a severe risk of reactor failure. Additionally, damage to support infrastructure, such as power lines and water supply systems, could compromise emergency response efforts, further increasing the risk of a nuclear accident.

A Comprehensive risk assessment is required to ensure the stability of foundations, especially for nuclear installations and other important buildings in areas at risk of liquefaction. This assessment includes laboratory and field tests to determine the physical and mechanical properties of the soil at relevant depths so that the liquefaction potential can be properly predicted [18]. Soil stabilization methods such as soil compaction, grouting and the installation of stone columns are important steps to strengthen the soil structure and reduce the risk of liquefaction [9]. The use of deep foundations to reach more stable soil layers is essential for the construction of liquefaction-resistant structures, especially for nuclear power plants where structural failure must be avoided at all costs. Additionally, effective drainage systems should be incorporated to reduce the saturated moisture level of soils, which is one of the main factors in liquefaction. In more general building construction, reducing ground loads through lighter building structures and more uniform load distribution can help maintain structural stability in weak areas. Additionally, the implementation of early warning systems with sensors and monitoring technologies is essential to detect early signs of liquefaction, so that emergency measures can be taken before significant damage occurs, especially in safety-critical nuclear power plants [5]. This integrated approach can minimize the risk of liquefaction and maintain the stability of foundations and building structures even under extreme seismic conditions.

Implications for nuclear safety and PSA integration

Engineering design response to liquefaction hazards

The design of Nuclear Power Plant (NPP) foundations in liquefaction-prone regions necessitates a thorough geotechnical strategy that provides structural stability and operational safety in the face of extreme seismic occurrences. In areas like Serpong, where shallow groundwater and alluvial deposits increase the risk of seismic-induced liquefaction, foundation systems must be designed to reduce differential settlement and lateral spreading. To ensure uniform load distribution and structural rigidity under seismic loading, standard nuclear engineering practices recommend the use of deep foundation systems, such as piled raft foundations or large mat foundations supported by end-bearing piles, anchored in non-liquefiable strata [8,9,21]. Furthermore, flexible pipe and cabling connections are required to accommodate potential ground deformations and prevent functional disruptions to safety-critical systems. These design considerations are consistent with the International Atomic Energy Agency's SSR-1 safety criteria, which require NPPs to be capable of performing safety functions even in the presence of considerable geotechnical hazards [8] that require all safety functions to remain operable even in degraded soil conditions.

Observations from real-world incidents

Empirical studies and real-world incidents have consistently highlighted the critical role of Soil-Structure Interaction (SSI) and Structure-Soil-Structure Interaction (SSSI) in nuclear site safety assessments under liquefaction conditions. For instance, liquefaction-induced ground deformations can amplify relative displacements among adjacent nuclear structures, as shown by recent investigations [22,23]. Even structurally sound facilities may experience differential settlement or tilting that compromises interconnected safety-critical systems such as emergency pipelines, electrical conduits, or shared basemat layouts. These findings emphasize the necessity of modeling complex geostructural responses in probabilistic seismic hazard assessments for nuclear installations [21].

Historical nuclear events have further validated these mechanisms. During the 2011 Fukushima Daiichi disaster, ground deformation disrupted emergency access and fuel supply lines, while in the 2007 Niigata-Chuetsu earthquake, liquefaction beneath transformer yards caused significant tilting and power loss despite intact reactors [24]. Beyond Japan, the 1995 Kobe earthquake revealed how liquefaction on reclaimed land resulted in severe structural misalignment, reinforcing the risks of SSSI even in non-nuclear facilities [25]. Similarly, the 2011 Christchurch earthquake in New Zealand and the 1999 Izmit earthquake in Turkey caused extensive damage to

underground lifelines and critical infrastructure, leading to global reassessment of geotechnical vulnerability in urban and industrial areas [26,27]. These cases underscore the necessity for nuclear safety frameworks to address not only structural performance but also system-level continuity and resilience against liquefaction-induced hazards.

Liquefaction-Induced functional failures in critical NPP systems

Liquefaction-induced ground displacement can cause severe failures in Nuclear Power Plant (NPP) systems via mechanisms that, while not directly compromising structural integrity, dramatically affect operation. These failures frequently emerge as secondary effects, including as differential settlement, lateral spreading, and ground tilting, which move into the operational domains of safety-critical systems. The most notable functional vulnerabilities are:

Control rod misalignment caused by tilting or uneven settlement of the reactor basemat, which may impede scram operations. This issue is especially important in Boiling Water Reactors (BWRs), because vertical rod motion is gravity-assisted. Experimental experiments [22] and post-earthquake assessments [24] show that even small tilting degrees (<1°) can cause considerable displacement at guide assemblies; Pipeline rupture, particularly at elbows, expansion joints, or flange couplings, caused by differential lateral movement over building borders or buried-above-ground interfaces. These vulnerabilities have been reported in a number of seismic occurrences, including the Niigata and Christchurch earthquakes, where liquefaction damaged emergency cooling and fire suppression lines [21,26]; Cable tray and conduit failure in underground or embedded networks owing to tensile stress or deformation caused by ground subsidence. Such failures have the potential to disrupt power supplies or instrumentation control circuits. The United States Nuclear Regulatory Commission [28] emphasizes the need to account for these impacts in the dependability modeling of support systems, particularly under seismic-induced deformation; Uneven settlement or tilting of base pads can cause diesel generator malfunctions by impairing fuel supply systems, misaligning coupling shafts, or causing vibration-induced shutdowns. Lessons from the Fukushima disaster indicate that partial loss of functionality in diesel systems due to flooding and foundation movement can result in cascading power failures across redundant trains [24].

These failure modes are especially pernicious because they can create common-cause failures across seemingly separate safety systems, breaking defense-in-depth principles. Redundant systems located on shared basemats or underground infrastructure are vulnerable to simultaneous disruption, reducing overall plant resilience.

International nuclear safety standards, such as IAEA SSG-9 [29] and NRC guidance [28], require that functional hazards be explicitly included in seismic design and probabilistic safety assessments. Flexible couplings, decoupled support systems, deep foundations that bypass liquefiable layers, and improved SSI modeling to capture non-linear soil-structure interaction effects are among the recommended mitigation strategies [30,31].

Integration into the Probabilistic Safety Assessment (PSA)

This study enables the inclusion of liquefaction hazard into the Level 1 and Level 2 PSA of nuclear facilities by taking the following steps:

Hazard quantification: The total liquefaction probability derived for various return durations are used to calculate the frequency of initiating events; Fragility modeling: Conditional probabilities for system-level failures (e.g., piping rupture, cable damage) can be combined with component fragilities; Risk metrics: The output can help calculate metrics like Core Damage Frequency (CDF) and Large Early Release Frequency (LERF).

Similar probabilistic frameworks have also been applied in nuclear safety assessments beyond external physical hazards, for example in evaluating the reliability of digital instrumentation and control systems such as reactor protection systems using Bayesian network models [Santoso et al., 2019] [32]. This integration supports the IAEA's SSG-3 [33] and SSG-4 [34] guidelines for integrating external hazard assessments to PSA outcomes, as well as promoting a risk-informed, uncertainty-aware approach to siting and design decisions in Indonesian NPP construction.

CONCLUSION

This study presents the first localized probabilistic liquefaction model applied to a installations site in Indonesia, addressing important seismic and geotechnical uncertainties in the Serpong region. We predict 50-year liquefaction probabilities ranging from 0.5676 to 0.594 by combining PSHA outputs, ground motion parameters, and subsurface soil heterogeneity. The findings suggest that shallow

saturated layers, particularly those at 1-6 m depth, represent significant threats to infrastructure, especially when magnitudes exceed 6.5 MW. These findings highlight the importance of site-specific mitigation, which includes deep foundations, drainage systems, and ground improvement. Importantly, the results are formatted for use in Probabilistic Safety Assessment (PSA) to assess risk indicators such as Core Damage Frequency (CDF) and Large Early Release Frequency (LERF). This study promotes risk-informed NPP design and regulatory planning by providing a replicable paradigm for future siting studies in Indonesia and other seismically active regions.

ACKNOWLEDGMENT

The authors gratefully acknowledge the Head of the Research Center for Nuclear Reactor Technology for providing financial support for the research activities conducted in 2023. The authors also sincerely acknowledge the Director of Talent Management for funding the *Degree by Research* scheme supporting the Doctoral Degree program at Universitas Indonesia, which substantially contributed to the completionof this study.

AUTHOR CONTR IBUTION

Akhmad Muktaf Haifani: Writing – original draft, Methodology, Investigation, Validation, Conceptualization, Visualization, Formal Analysis, Funding acquisition, Widjojo Prakoso: Supervision, Conceptualization, Writing – review & editing, Formal Analysis, Topan Setiadipura: Methodology, Validation, Supervision, Conceptualization, Hadi Suntoko: Validation, Conceptualization, Formal Analysis, Writing - review & editing, Adi Gunawan Muhammad: Methodology, Investigation, Conceptualization, Formal Analysis.

REFERENCE

1. Pusat Penelitian dan Pengembangan Geologi, Peta Rawan Bencana Gempa Bumi, Skala 1:10.000.000, P. P. Geologi, Bandung (2004). (in Indonesian)
2. Badan Tenaga Nuklir Nasional, Site Evaluation Report of RDE on Seismic Aspect, BATAN, Jakarta (2016). (in Indonesian)
3. T. Turkandi, Peta Geologi Lembar Jakarta dan Kepulauan Seribu, Jawa, Pusat Penelitian dan Pengembangan Geologi, Bandung (1992). (in Indonesian)
4. Badan Standardisasi Nasional (BSN), Tata Cara Perencanaan Ketahanan Gempa untuk Struktur Bangunan Gedung dan Non Gedung, SNI 1726, BSN, Jakarta (2012). (in Indonesian)
5. T. L. Youd and I. M. Idriss, J. Geotech. Geoenviron. Eng. **127** (2001) 297.
6. C. H. Juang, T. Jiang, and R. D. Andrus, J. Geotech. Geoenviron. Eng. **128** (2002) 580.
7. K. Tokimatsu, and H. B. Seed, Simplified Procedures for The Evaluation of Settlements in Clean Sands, National Technical Information Service, Earthquake Engineering Research Center, University of California, Berkeley (1984) 1.
8. International Atomic Energy Agency (IAEA), Site Evaluation for Nuclear Installations, Specific Safety Requirements SSR-1, IAEA, Vienna 2019
9. I. M. Idriss dan R. W. Boulanger, Soil Liquefaction During Earthquake, University of California, Barkeley (2010) 1.
10. H. B. Seed and I. M. Idriss, Ground Motions and Soil Liquefaction During Earthquakes, Earthquake Engineering Research Institute (EERI), Berkeley (1982) 134.
11. N. N. Ambraseys, Earthq. Eng. Struct. Dyn. **17** (1988) 1.
12. I. Arango, J. Geotech. Eng. **122** (1996) 929.
13. R. D. Andrus and K. H. Stokoe, *Liquefaction Resistance Based on Shear-Wave Velocit,* in: Proceedings of the NCEER Workshop on Evaluation of Liquefaction Resistance of Soils, National Center for Earthquake Engineering Research (NCEER), New York (1997) 89.
14. S. K. Youd, T. L, and Noble, *Magnitude Scaling Factors*, in: Proceedings of the NCEER Workshop on Evaluation of Liquefaction Resistance of Soils*,* National Center for Earthquake Engineering Research, State University of New York at Buffalo,New York (1997) 149.
15. R. W. Boulanger and I. M. Idriss, J. Geotech. Geoenviron. Eng. **142 (**2016) 1.
16. P. K. Robertson and C. E. Wride, Can. Geotech. J., **35** (1998) 442.
17. T. L. Youd, Liquefaction-Induced Lateral Spreading Displacement, Naval Civil Engineering Laboratory (NCEL), California **(**1993).

18. Steven L. Kramer, Geotechnical Earthquake Engineering, Prentice-Hall. Inc, New Jersey (1996).

19. S. L. Kramer and R. T. Mayfield, J. Geotech. Geoenviron. Eng**. 133** (2007) 802.

20. K. O. Cetin and R. B. Seed, Soil Dyn. Earthq. Eng. **24** (2004) 103.

21. R. Luque and J. D. Bray, Soil Dyn. Earthq. Eng. **133** (2020) 106026.

22. J. P. Stewart, A. H. Liu, and Y. Choi, Bull. Seismol. Soc. Am. 93 (2003) 332.

23. T. J. Katona, Z. Bán, E. Győri *et al*., Sci. Technol. Nucl. Install. **2015 (**2015) 1.

24. Tokyo Electric Power Company (TEPCO), Fukushima Nuclear Accidents Investigation Report (Attachment 2): List of Documents concerning the Response Status at Fukushima Daiichi Nuclear Power Station and Fukushima Daini Nuclear Power Station, TEPCO, Tokyo, 2012.

25. K. Tokimatsu and Y. Asaka, Soils Found. **38** (1998) 163.

26. M. Cubrinovski, J. D. Bray, M. Taylor *et al.*, Seismol. Res. Lett. **82** (2011) 893.

27. A. Karakaş and Ö. Coruk, Environ. Eng. Geosci. **16** (2010) 411.

28. R. K. McGuire, W. J. Silva, and C. J. Costantino, Technical basis for revision of regulatory guidance on design ground motions: development of hazard-and risk-consistent seismic spectra for two sites, U.S. Nuclear Regulatory Commission (NRC), Washington D.C (2002).

29. International Atomic Energy Agency (IAEA), Seismic Hazards in Site Evaluation for Nuclear Installations, Specific Safety Guide: No. SSG-9 Rev.1, IAEA, Vienna, 2022.

30. R. W. Boulanger and I. M. Idriss, CPT and SPT based liquefaction triggering procedures, Center for Geotechnical Modeling Department of Civil and Environmental Engineering, University of California, California (2014) 1.

31. J.-H. Hwang, C.-H. Chen, and C. H. Juang, *Liquefaction Hazard Analysis: A Fully Probabilistic Method*, in: Geo-Frontiers 2005 Congress, American Society of Civil Engineers (ASCE) (2005) 1.

32. S. Santoso, S. Bakhri, and J. Situmorang, Atom Indones. **45** (2019) 43.

33. International Atomic Energy Agency. (IAEA), Development and Application of Level 1 Probabilistic Safety Assessment for Nuclear Power Plants, Specific Safety Guide No. SSG-3, IAEA, Vienna, 2010

34. International Atomic Energy Agency. (IAEA), Development And Application of Level 1 Probabilistic Safety Assessment for Nuclear Power Plants, IAEA Safety Standards No. SSG-3, Rev. 1. IAEA, Vienna, 2024

35. D. Monelli, M. Pagani, G. Weatherill *et al., The Hazard Component of Openquake: The Global Earthquake Model's Calculation Engine*, in: Proceedings of the 15th World Conference on Earthquake Engineering, Lisbon (2012) 24.

36. T. Iwasaki, K. Tokida, and F Tatsuoka, *Soil Liquefaction Potential Evaluation with Use of The Simplified Procedure,* in: Proceedings of the 1st International Conference on Recent Advances in Geotechnical Earthquake Engineering and Soil Dynamics, St. Louis, (1981) 209.

37. M. Budhu, Soil Mechanics And Foundations, 3rd Edition, John Wiley & Sons, Hoboken (2010)